

# Ionic Liquid-assisted Synthesis of Polyaniline/Gold Nanocomposite and Its Biocatalytic Application

Wenrong Yang · Jingquan Liu · Rongkun Zheng ·  
 Zongwen Liu · Yun Dai · Guonan Chen ·  
 Simon Ringer · Filip Braet

Received: 21 August 2008 / Accepted: 25 September 2008 / Published online: 15 October 2008  
 © to the authors 2008

**Abstract** In this report, a novel chemical synthesis of polyaniline/gold nanocomposite is explored using ionic liquid (IL) 1-Butyl-3-methylimidazolium hexafluorophosphate. The direct chemical synthesis of polyaniline/gold nanocomposite was initiated via the spontaneous oxidation of aniline by  $\text{AuCl}_4^-$  in IL. A nearly uniform dispersion of polyaniline/Au particles with a diameter of  $450 \pm 80$  nm was produced by this method, which indicates that this method is more suitable for controlling particle dimensions. It was also found that the electrical conductivity of the polyaniline/gold nanocomposite was more than 100 times higher than that of the pure polyaniline nanoparticles. The polyaniline/gold nanocomposite displays superior function in the biocatalytic activation of microperoxidase-11

because of the high surface area of the assembly and the enhanced charge transport properties of the composite material. We also report the possible application of polyaniline/gold nanocomposite as a  $\text{H}_2\text{O}_2$  biosensor.

**Keywords** Ionic liquid · Nanocomposite · Biocatalytic application

## Introduction

Electrically conducting polymers have attracted attention for applications in various electrochemical devices including batteries [1], capacitors [2], electrochromic windows [3], displays [3], actuators [4, 5], photovoltaic cells [6], electrochemical biofuel cells [7], and biosensors [8]. Polyaniline is one of the most useful conducting polymers due to its facile synthesis, environmental stability, and simple acid/base doping/dedoping chemistry [9]. Room-temperature ionic liquids (ILs) [10] are organic salts with melting points near room temperature, which are regarded as environmentally friendly benign solvents because of their nonvolatility and high stability. The advantages of ILs in synthetic processes of functional materials have been gradually realized and have received more and more attention. ILs have widely been used in organic synthesis, electrochemistry, catalysis, and separation, but synthesis of nanostructured materials in ILs is relatively new and has been attracting growing interest in recent years. By using ILs as a reaction media, some nanostructured materials, such as gold nanoparticles [11, 12], mesoporous materials [13], hollow microspheres [14–17], CuCl nanosheetlets [18, 19], CoPt nanorods [20], and polymer nanoparticles [21, 22] have been successfully synthesized. The potential benefits of using ILs as reaction media for conducting polymers are

W. Yang (✉) · R. Zheng · Z. Liu · S. Ringer · F. Braet  
 Australian Key Centre for Microscopy & Microanalysis,  
 The University of Sydney, Sydney, NSW 2006, Australia  
 e-mail: w.yang@usyd.edu.au

Z. Liu (✉)  
 e-mail: z.liu@usyd.edu.au

J. Liu  
 School of Chemical Science and Engineering, The University  
 of New South Wales, Sydney, NSW 2005, Australia

Y. Dai  
 School of Chemistry and Biotechnology, Yunnan Institute  
 of Nationalities, Kunming, Yunnan, People's Republic of China

G. Chen  
 Ministry of Education Key Laboratory of Analysis and Detection  
 for Food Safety, Fuzhou University, Fuzhou, Fujian 350002,  
 China

G. Chen  
 Department of Chemistry, Fuzhou University, Fuzhou,  
 Fujian 350002, China

drawing increasing attention [23]. Hybrid systems consisting of metallic or semiconducting nanoparticles and organic compounds became an interesting research topic in recent years [24] and have stimulated substantial research efforts directed to the development of hybrid materials of new catalytic, electronic, and optoelectronic functionalities [25, 26]. In particular, the incorporation of metallic or semiconducting nanoparticles in conductive redox polymers, such as polypyrrole and polyaniline, is of interest because of strong electronic interactions between the nanoparticles and the polymer matrixes. The ability to control the shape and size of nanocomposites is an important factor for defining their properties, such as the electronic band gap, conductivity, and light-emission efficiency [27].

Recently, it was found that chloroaurate ions ( $\text{AuCl}_4^-$ ) could also be applied as an oxidant in the oxidative polymerization of pyrrole, leading to gold nanostructures capped with polypyrrole [28, 29]. Sastry and co-authors [30, 31] demonstrated that  $\text{AuCl}_4^-$  could be reduced by amine-containing molecules including hexadecylaniline and diamine-containing oxyethylene linkage, resulting in metallic gold particles accompanied with the formation of corresponding polymers. In this present work, we studied the oxidative polymerization of aniline using  $\text{HAuCl}_4$  as the oxidant and 1-Butyl-3-methylimidazolium hexafluorophosphate as the growth media that resulted in the formation of the polyaniline/gold nanocomposite. It was found that the polyaniline/gold nanocomposite possesses enhanced electrochemical activity and superior conductivity compared to the conducting polymers prepared by the conventional approach. In addition, the polyaniline/gold nanocomposite was used to immobilize microperoxidase-11 (MP-11) and its biocatalytic properties were also investigated. It was found that MP-11 could be easily immobilized with high loading and activity because of the large specific surface area, excellent conductivity, and strong interaction between the polyaniline/gold nanocomposite and MP-11. Furthermore, the small dimensions and the high surface-to-volume ratio of the nanocomposite allow the electrons transmit rapidly and hence enhance current response. Thus, the polyaniline/gold nanocomposite can be used as an excellent matrix for electrocatalysis and enzyme immobilization. The aim of the present study is to develop a novel type of electrode material for using in hydrogen peroxide biosensor [32, 33] and biofuel cell [34].

## Experimental Section

All chemicals were of analytical grade and used as received. 1-Butyl-3-methylimidazolium hexafluorophosphate was purchased from Sigma-Aldrich. MP-11 was

obtained from Sigma and used as received. Aniline was distilled twice under atmospheric pressure and stored in dark at low temperature prior to use. Hydrochloric acid and other reagents were used without further purification. All aqueous solutions were prepared using Mill-Q water.

In a typical synthesis, 0.2 g of aniline was dissolved in 10 mL of IL, and 0.1 g of  $\text{HAuCl}_4 \cdot 3\text{H}_2\text{O}$  was dissolved in 10 mL water with 0.5 mL hydrochloric acid (1 M HCl). The two solutions were then carefully transferred to a glass tube, and an interface was formed between the aqueous phase and the 1-Butyl-3-methylimidazolium hexafluorophosphate. After 5 min, green polyaniline formed at the interface and then gradually diffused into the aqueous phase. After 24 h, the entire water phase was filled homogeneously with dark-green polyaniline/gold nanocomposite. The aqueous phase was then collected, and washed with ethanol and water to remove the unreacted chemicals and aniline oligomers. The obtained polyaniline/gold nanocomposite was dried in a vacuum oven at 40 °C for 24 h.

Transmission electron microscopy (TEM) characterization was performed with a Philips CM12. All the electrochemical experiments were carried out with a BAS 100B electrochemical workstation (USA). A conventional three-electrode system comprising a bare or modified glassy carbon electrode (GCE) as the working electrode, a platinum foil as the auxiliary, and an Ag/AgCl/3.0 M NaCl electrode (from BAS) as the reference. The GCE (3 mm in diameter) was polished with 1.0, 0.3, and 0.05  $\mu\text{m}$  alumina slurry followed by rinsing with doubly distilled water and drying at room temperature. XP spectra were obtained using an EscaLab 220-IXL spectrometer with a monochromated Al K $\alpha$  source (1486.6 eV), a hemispherical analyzer and a multichannel detector. The spectra were accumulated at a take-off angle of 90° with a 0.79 mm<sup>2</sup> spot size at a pressure of less than 10<sup>−8</sup> mbar.

The polyaniline/gold nanocomposite was dispersed in Mill-Q water and an amount of 10  $\mu\text{L}$  of the solution was coated on the surface of GCE. The surface coverage of the nanocomposite was about  $2.8 \times 10^{-6}$  g/cm<sup>2</sup>. Subsequently, the electrode was thoroughly rinsed with water and immersed in a 1 mg mL<sup>−1</sup> MP-11 in 0.1 M phosphate buffer solution (PBS, pH 7.0) at 4 °C for 10 h to obtain MP-11/polyaniline/gold nanocomposite electrodes. The electrode was thoroughly rinsed with Mill-Q water before each experiment. The enzyme electrodes were kept in PBS at 4 °C when not in use. The PBS buffers were purged with purified nitrogen for 20 min prior to a series of electrochemical experiments. A nitrogen environment was kept over solutions in the cell to keep them oxygen free. A 10 mM  $\text{H}_2\text{O}_2$  solution was prepared by adding 0.12 mL of the 30%  $\text{H}_2\text{O}_2$  solution to 4.8 mL of PBS Buffer. Once diluted, the  $\text{H}_2\text{O}_2$  should be used promptly, as it degrades rapidly.

## Results and Discussion

In this report, a polyaniline/gold nanocomposite was produced by polymerization of aniline using chloroaurate acid ( $\text{HAuCl}_4$ ) as the oxidant in water/ILs interface. Both water and ILs are environmental benign solvents. The reduction of  $\text{AuCl}_4^-$  was accompanied by oxidative polymerization of aniline, leading to the formation of uniform submicron sized composite particles ( $450 \pm 80$  nm in diameter, Fig. 1) of polyaniline and gold. The mechanism of the formation of the polyaniline/gold nanocomposite is not clear so far. It is known that aniline is protonated in acidic solution. Therefore, in the experiment, when aniline acidic solution was mixed with chloroaurate acid, the protonated aniline was first electrostatically complexed with  $\text{AuCl}_4^-$ , and then reduction of  $\text{HAuCl}_4$  and oxidation of aniline occurred simultaneously, leading to the formation of the polyaniline/gold nanocomposite.

The present method of synthesis is similar to other routes with the exception of using chloroaurate acid as an oxidant in ILs, and the products possess similar chemical structure but different morphology and improved conductivity. Previously, Wang et al. [35] demonstrated a facile route to the synthesis of polyaniline nanofibers by polymerization of aniline using chloroaurate acid ( $\text{HAuCl}_4$ ) as the oxidant. Clearly the morphology of the polyaniline/gold nanocomposite based on the present method is quite different from that of the previous work. Also the conductivity of the polyaniline/gold nanocomposite was found to be 0.12 S/cm, whereas that of polyaniline was found to be  $2.4 \times 10^{-3}$  S/cm [36]. Thus, there was an increase of

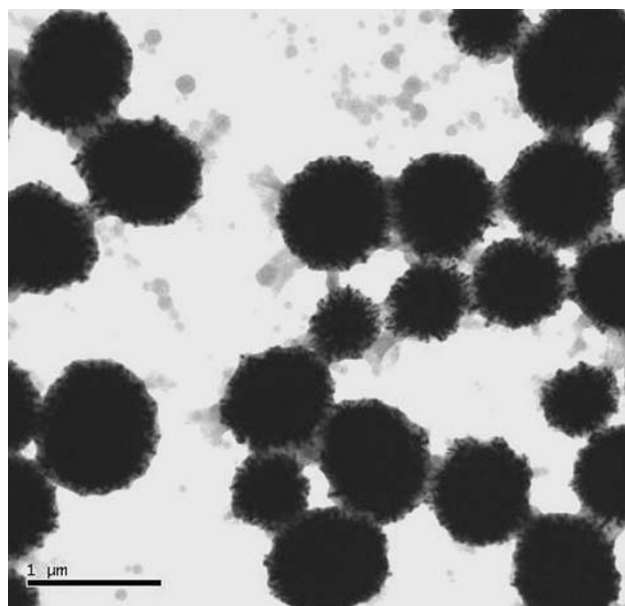


**Fig. 1** TEM micrograph of the polyaniline/gold nanocomposite prepared by the present method. Scale bar is 1  $\mu\text{m}$

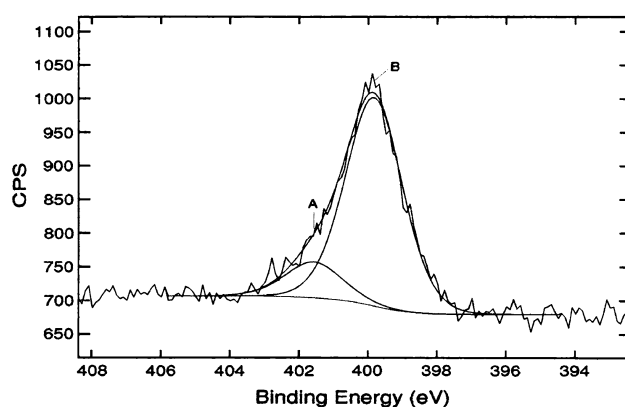


**Fig. 2** The X-ray photoelectron spectra of the N 1s for the polyaniline/gold nanocomposite. The peak A at binding energy of 399.4 eV corresponds to the benzenoid amine ( $-\text{NH}-$ ). A higher binding energy peak (Peak B) centered at 401.2 eV is also found in Au–Polyaniline

about three orders of magnitude in conductivity upon incorporation of gold in the conductive form of polyaniline prepared using the present method. Because gold is a conductor, it is beneficial for improving the conductivity of polyaniline when it is combined with gold. Therefore, with increasing gold content, the conductivity of the polyaniline/gold nanocomposite should be enhanced.

The polyaniline/gold nanocomposite was further characterized by XPS and the core level spectrum of N 1s is shown in Fig. 2. The peak at binding energy of 399.4 eV corresponds to the benzenoid amine ( $-\text{NH}-$ ). A higher binding energy peak centered at 401.2 eV is also found. This high binding energy peak is attributed to the positively charged nitrogen ( $\text{N}^+$ ), indicating that the polyaniline/gold nanocomposite was in the doped state (the emeraldine salt form). The oxidation state of the incorporated gold was determined by XPS analysis which revealed the presence of Au(0) only in the nanocomposite.

As reported before, MP-11 immobilized on gold electrodes can catalyze the reduction of  $\text{H}_2\text{O}_2$  [34, 37, 38]. In the present work, the reduction of  $\text{H}_2\text{O}_2$  was also investigated using the modified polyaniline/gold nanocomposite electrode. Figure 3 shows cyclic voltammograms of the polyaniline/gold nanocomposite electrode in 0.1 M PBS (pH 7.0) in the absence and presence of  $\text{H}_2\text{O}_2$  at a scan rate of 20 mV/s. In the absence of  $\text{H}_2\text{O}_2$ , a pair of the redox peaks of MP-11 was observed, which is similar to that observed by Gorton et al. [38]. In the presence of  $\text{H}_2\text{O}_2$ , however, the voltammetric behavior changed drastically. A large cathodic current for the reduction of  $\text{H}_2\text{O}_2$  appeared while the anodic peak decreased till it disappeared completely. A current–time plot of the enzyme electrode on successive step changes of  $\text{H}_2\text{O}_2$  concentration is displayed in Fig. 4. When an aliquot of  $\text{H}_2\text{O}_2$  was added into the buffer solution, the reduction current rose steeply to reach a

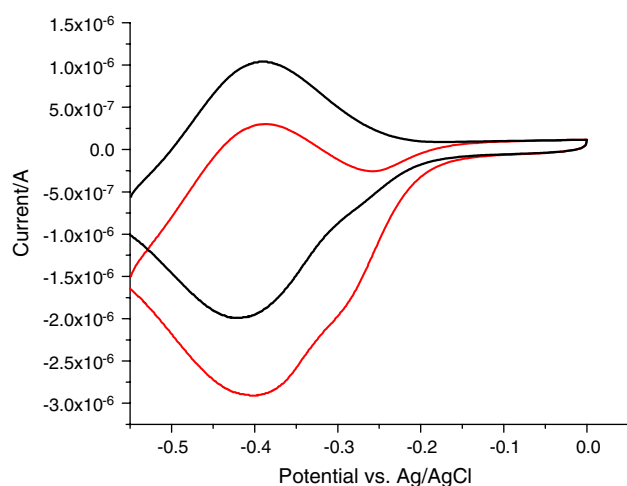


**Fig. 3** Cyclic voltammograms of polyaniline/gold nanocomposite electrode in 0.1 M PBS (pH 7.0) without and with 1 mM  $\text{H}_2\text{O}_2$  concentration at 20 mVs. In the absence of  $\text{H}_2\text{O}_2$ , a pair of the redox peaks of MP-11 was observed, the voltammetric behavior changes drastically in the presence of  $\text{H}_2\text{O}_2$

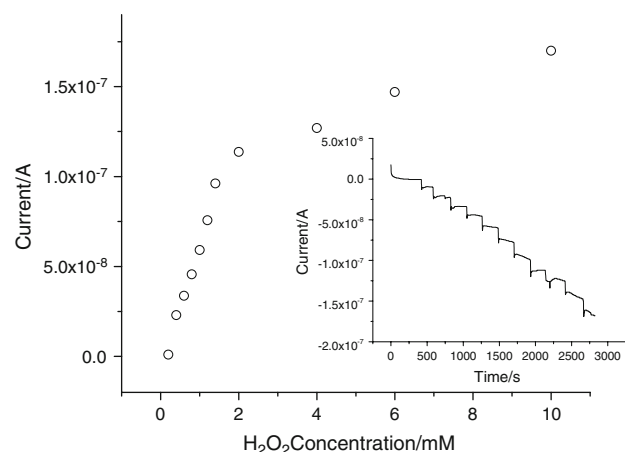


**Fig. 4** Calibration curve for the determination of  $\text{H}_2\text{O}_2$  at the polyaniline/gold nanocomposite electrode. Applied potential:  $-400$  mV, supporting electrolyte: 0.1 M pH 7.0 PBS with  $\text{N}_2$ -saturated. Inset: typical steady-state response of the biosensor on successive injection of  $\text{H}_2\text{O}_2$  into stirring PBS

stable value and the response time was less than 10 s, which indicated a fast biocatalytic and diffusion process and a high activity of the MP-11 in this enzyme/nano-structured hybrid system (Fig. 4). The linear range of  $\text{H}_2\text{O}_2$  concentration is between 2.0 mM and 20  $\mu\text{M}$  with a correlation coefficient of 0.99 (Fig. 4). The modified polyaniline/gold nanocomposite electrode has a detection limit of 0.8  $\mu\text{M}$  at a signal-to-noise ratio of 3. In addition, the long-term stability of the polyaniline/gold nanocomposite electrode was investigated over a 10-day period. When the modified electrode was stored at 4  $^\circ\text{C}$  and measured intermittently, no apparent change in the

response to 0.1 mM  $\text{H}_2\text{O}_2$  was found over this period. The observed stability could be attributed to the strong interactions between the polyaniline/gold nanocomposite and MP-11, which obviously indicates that MP-11 was firmly immobilized on the surface of the polyaniline/gold nanocomposite films.

## Conclusions

In summary, the polyaniline/gold nanocomposite has been successfully prepared by employing chloraurate ions as the oxidant in ILs. The direct electrochemistry of MP-11, modified on microelectrode, and its catalytic activity for the reduction of  $\text{H}_2\text{O}_2$  were studied by CV. A pair of well-defined redox waves corresponding to the conversion of MP-Fe(III) and MP-Fe(II) was obtained, which demonstrates that the polyaniline/gold nanocomposite has a good promotion toward the reduction/oxidation of MP-11. The high conductivity, large specific surface area, and excellent electroactivity of the polyaniline/gold nanocomposite make it an excellent matrix for enzyme immobilization and electrocatalysis. When combined with MP-11, the nanocomposite electrode displays a potential application for the detection of  $\text{H}_2\text{O}_2$  with a low detection limit and rapid response time. Moreover, the nanocomposite-modified electrode exhibits high stability.

**Acknowledgments** The authors acknowledge the facilities as well as scientific and technical assistance from staff in the Australian Microscopy & Microanalysis Research Facility (AMMRF) at the Australian Key Centre for Microscopy and Microanalysis at the University of Sydney.

## References

1. B. Winther-Jensen, O. Winther-Jensen, M. Forsyth, D.R. MacFarlane, *Science* **321**, 671–674 (2008). doi:[10.1126/science.1159267](https://doi.org/10.1126/science.1159267)
2. C. Peng, S.W. Zhang, D. Jewell, G.Z. Chen, *Prog. Nat. Sci.* **18**, 777–788 (2008). doi:[10.1016/j.pnsc.2008.03.002](https://doi.org/10.1016/j.pnsc.2008.03.002)
3. W. Lu, A.G. Fadeev, B.H. Qi, B.R. Mattes, *J. Electrochem. Soc.* **151**, H33–H39 (2004). doi:[10.1149/1.1640635](https://doi.org/10.1149/1.1640635)
4. W. Lu, A.G. Fadeev, B.H. Qi, E. Smela, B.R. Mattes, J. Ding, G.M. Spinks, J. Mazurkiewicz, D.Z. Zhou, G.G. Wallace, D.R. MacFarlane, S.A. Forsyth, M. Forsyth, *Science* **297**, 983–987 (2002). doi:[10.1126/science.1072651](https://doi.org/10.1126/science.1072651)
5. W. Lu, A.G. Fadeev, B. Qi, B.R. Mattes, *Synth. Met.* **135**, 139–140 (2003). doi:[10.1016/S0379-6779\(02\)00558-1](https://doi.org/10.1016/S0379-6779(02)00558-1)
6. P. Suresh, P. Balaraju, S.K. Sharma, M.S. Roy, G.D. Sharma, *Sol. Energy Mater. Sol. Cells* **92**, 900–908 (2008). doi:[10.1016/j.solmat.2008.02.028](https://doi.org/10.1016/j.solmat.2008.02.028)
7. I. Willner, G. Arad, E. Katz, *Bioelectrochem. Bioenerg.* **44**, 209–214 (1998). doi:[10.1016/S0302-4598\(97\)00091-3](https://doi.org/10.1016/S0302-4598(97)00091-3)
8. J.J. Gooding, L. Pugliano, D.B. Hibbert, P. Erokhin, *Electrochem. Commun.* **2**, 217–221 (2000). doi:[10.1016/S1388-2481\(00\)00035-5](https://doi.org/10.1016/S1388-2481(00)00035-5)

9. A.G. MacDiarmid, *Angew. Chem. Int. Ed.* **40**, 2581–2590 (2001). doi:10.1002/1521-3773(20010716)40:14<2581::AID-ANIE2581>3.0.CO;2-2
10. T. Welton, *Chem. Rev.* **99**, 2071–2083 (1999). doi:10.1021/cr980032t
11. E. Dinda, S. Si, A. Kotal, T.K. Mandal, *Chem. Eur. J.* **14**, 5528–5537 (2008). doi:10.1002/chem.200800006
12. Y. Qin, Y. Song, N.J. Sun, N. Zhao, M.X. Li, L.M. Qi, *Chem. Mater.* **20**, 3965–3972 (2008). doi:10.1021/cm8002386
13. B.G. Trewyn, C.M. Whitman, V.S.Y. Lin, *Nano Lett.* **4**, 2139–2143 (2004). doi:10.1021/nl048774r
14. H. Luo, C. Xu, D.B. Zou, L. Wang, T.K. Ying, *Mater. Lett.* **62**, 3558–3560 (2008). doi:10.1016/j.matlet.2008.03.050
15. T. Nakashima, N. Kimizuka, *J. Am. Chem. Soc.* **125**, 6386–6387 (2003). doi:10.1021/ja034954b
16. C. Xu, L. Wang, H. Luo, D.B. Zou, T.K. Ying, *Chin. J. Inorg. Chem.* **23**, 1941–1946 (2007)
17. F.B. Zhang, H.L. Li, *Mater. Chem. Phys.* **98**, 456–458 (2006). doi:10.1016/j.matchemphys.2005.09.063
18. A. Taubert, *Angew. Chem. Int. Ed.* **43**, 5380–5382 (2004). doi:10.1002/anie.200460846
19. A. Taubert, *Acta Chim. Slov.* **52**, 183–186 (2005)
20. Y. Wang, H. Yang, *J. Am. Chem. Soc.* **127**, 5316–5317 (2005). doi:10.1021/ja043625w
21. H.X. Gao, T. Jiang, B.X. Han, Y. Wang, J.M. Du, Z.M. Liu, J.L. Zhang, *Polymer* **45**, 3017–3019 (2004). doi:10.1016/j.polymer.2004.03.002
22. Z.J. Miao, Y. Wang, Z.M. Liu, J. Huang, B.X. Han, Z.Y. Sun, J.M. Du, *J. Nanosci. Nanotechnol.* **6**, 227–230 (2006). doi:10.1166/jnn.2006.151
23. J.M. Pringle, O. Winther-Jensen, C. Lynam, G.G. Wallace, M. Forsyth, D.R. MacFarlane, *Adv. Funct. Mater.* **18**, 2031–2040 (2008). doi:10.1002/adfm.200701147
24. I. Willner, E. Katz, *Angew. Chem. Int. Ed.* **39**, 1181–1218 (2000)
25. P. Gomez-Romero, *Adv. Mater.* **13**, 163–174 (2001). doi:10.1002/1521-4095(200102)13:3<163::AID-ADMA163>3.0.CO;2-U
26. W.R. Yang, B. Raguse, G. Stockton, unpublished results (2008)
27. J.X. Huang, S. Virji, B.H. Weiller, R.B. Kaner, *J. Am. Chem. Soc.* **125**, 314–315 (2003). doi:10.1021/ja028371y
28. J. Njagi, S. Andreescu, *Biosens. Bioelectron.* **23**, 168–175 (2007). doi:10.1016/j.bios.2007.03.028
29. J. Njagi, J. Warner, S. Andreescu, *J. Chem. Educ.* **84**, 1180–1182 (2007)
30. P. Selvakannan, S. Mandal, R. Pasricha, M. Sastry, *J. Colloid Interface Sci.* **279**, 124–131 (2004). doi:10.1016/j.jcis.2004.06.027
31. P.R. Selvakannan, P.S. Kumar, A.S. More, R.D. Shingte, P.P. Wadgaonkar, M. Sastry, *Langmuir* **20**, 295–298 (2004). doi:10.1021/la0350352
32. M.K. Wang, F. Zhao, Y. Liu, S.J. Dong, *Biosens. Bioelectron.* **21**, 159–166 (2005). doi:10.1016/j.bios.2004.08.012
33. J.J. Gooding, P. Erokhin, D. Losic, W. Yang, V. Policarpio, J. Liu, F.M. Ho, M. Situmorang, D.B. Hibbert, J.G. Shapter, *Anal. Sci.* **17**, 3–9 (2001). doi:10.2116/analsci.17.3
34. I. Willner, E. Katz, F. Patolsky, A.F. Buckmann, *J. Chem. Soc., Perkin Trans. 2*, 1817–1822 (1998). doi:10.1039/a801487f
35. Y. Wang, Z.M. Liu, B.X. Han, Z.Y. Sun, Y. Huang, G.Y. Yang, *Langmuir* **21**, 833–836 (2005). doi:10.1021/la047442z
36. T.K. Sarma, D. Chowdhury, A. Paul, A. Chattopadhyay, *Chem. Commun.* 1048–1049 (2002). doi:10.1039/b201014c
37. F. Patolsky, E. Katz, V. Heleg-Shabtai, I. Willner, *Chem. Eur. J.* **4**, 1068–1073 (1998). doi:10.1002/(SICI)1521-3765(19980615)4:6<1068::AID-CHEM1068>3.0.CO;2-Q
38. L. Gorton, A. Lindgren, T. Larsson, F.D. Munteanu, T. Ruzgas, I. Gazaryan, *Anal. Chim. Acta* **400**, 91–108 (1999). doi:10.1016/S0003-2670(99)00610-8